Chapter 3

Tungsten Carbide as an Addition to High Speed Steel Based Composites

Marcin Madej

Additional information is available at the end of the chapter

http://dx.doi.org/10.5772/51243

1. Introduction

Design criteria for high strength tool materials have to include wear resistance of the abrasive particle, high hardness and adequate toughness. Cold compaction and vacuum sintering of PM high speed steels (HSSs) to full density is now a well established technique [1-3]. In recent years, work has been undertaken to sinter metal matrix composites that contain ceramic particles in HSSs by the same route. Most studies have focused on sintering with additions of hard ceramics such as Al_20_3, VC, NbC, TiC, WC and TiN with the aim of producing a more wear resistant HSS type material [4-18]. These composite materials have been developed for wear resistance applications as attractive alternative to the more expensive cemented carbides. Compared with high strength steels, these composite materials have higher hardness, wear resistance and elastic modulus. However, depending on size and distribution, the addition of brittle ceramic particles may cause degradation of bend strength and toughness owing to the initiation of cracks at or near the reinforcing particles. In order to ensure good bonding at the ceramic/matrix interfaces, the ceramic particles must exhibit some reactivity with the matrix. In contrast to Al_2O_3, which presents no interface reactions with the iron matrix, the diffusion of iron from the matrix into the MC carbide particles establishes a good cohesion across the ceramic/matrix interface. Besides, these carbides are stable in contact with iron during sintering and do not dissolve extensively. Therefore, MC particles were chosen as the reinforcement. A cheap and easy route to develop high speed steels reinforced with MC carbides consists of mixing powders of commercial high speed steel powders with the carbides.

There are two methods by which tungsten carbide powders are produced from the tungsten-bearing ores. Traditionally, tungsten ore is chemically processed to ammonium paratungstate and tungsten oxides. These compounds are then hydrogen-reduced to tungsten metal powder. The fine tungsten powders are blended with carbon and heated in a

hydrogen atmosphere between 1400 and 1500 °C (2500 and 2700 °F) to produce tungsten carbide particles with sizes varying from 0.5 to 30 μm. Each particle is composed of numerous tungsten carbide crystals. Small amounts of vanadium, chromium, or tantalum are sometimes added to tungsten and carbon powders before carburization to produce very fine (<1 μm) WC powders. In a more recently developed and patented process, tungsten carbide is produced in the form of single crystals through the direct reduction of tungsten ore (sheelite). The melting point of hexagonal tungsten carbide WC is equal to ~2780°C which is less than melting point of nonstoichiometric TiC, ZrC, HfC, NbC, and TaC carbides [1,2]. Hardness of tungsten carbide WC is equal to 18-22 GPa at room temperature which is less than that of nonstoichiometric TiC*y*, ZrC*y*, HfC*y*, VC*y*, NbC*y* and TaC*y* carbides [1, 2]. However, the hardness of WC is sufficiently stable in a wide temperature interval. For example, the microhardness *H*V of hexagonal WC carbide decreased from ~18 to ~12GPa at heating from room temperature to 1000°C whereas the HV of nonstoichiometric transition metal carbides decreased under the same conditions from their maximum values to 3-8GPa. A thermal expansion coefficient of WC is equal to ~$5.5 \cdot 10^{-6}$ K^{-1} [4-10] and is half as much as that of other transition metal carbides.

Metal matrix composites MMC have appeared as a bright option for wear applications. These materials combine a soft metallic matrix with hard ceramic particles that withstand wear. Different matrixes were studied, and aluminum, stainless steel and high speed steel HSS. Matrix composites showing outstanding wear behaviour. High hardness, mechanical strength, heat resistance and wear resistance of high speed steel (HSS) make it an attractive material for manufacture MMC. High speed steels comprise a family of alloys mainly used for cutting tools. Their name – high speed steel – is a synthesis of the following two features [11]:

a. the alloys belong to the Fe–C–X multicomponent system, where X represents a group of alloying elements in which Cr, W or Mo, V, and Co are the principal ones;
b. the alloys are characterized by their capacity to retain a high level of hardness even when submitted to elevated temperatures resulting from cutting metals at high speed.

The carbides are predominantly formed from the strong carbide formers V, W, Mo and Cr. Depending on the composition and on the thermal parameters (sintering temperature and cooling rate) several types of carbides can be formed. The main types are M_6C, M_2C, MC and $M_{23}C_6$. Their formation is a result of cooling rate and alloy composition. The carbides can be formed directly from the melt during solidification, by eutectic reaction or by decomposition of other types of carbide. The latter case can be seen from the decomposition of M_2C carbide into M_6C and MC carbides when HSS is annealed at temperatures above 1000°C. The importance of the alloying elements in HSS is the effect they have on the type of carbide formed and the temperature of formation, and also the effect they have on the tempering of martensite. The types of carbides are different in crystal structure and composition. The carbides MC, M_6C and $M_{23}C_6$ have a fcc crystal structure, while the metastable M_2C has a hcp structure. The carbides are also different in composition with higher V and Ti levels and

lower Fe and Cr levels in MC compared with M_6C and M_2C, which are rich in Mo and W. The carbide $M_{23}C_6$ is Cr rich, with high solubility for Fe and low solubility for W and Mo. Iron can substitute Cr when W and Mo are dissolved in this carbide. Annealed HSS generally contains $M_{23}C_6$. Considering HSS grades such as M3/2 it is clear that primary M_6C formation and growth along cell boundaries is a key problem. If the M_6C formation can be limited, while sintering to near full density is maintained, an acceptable final microstructure can result. The alloy composition of HSS may favour the formation of a certain type of carbide. For a given amount of V, increasing the amount of W favours the formation of M_6C at the expense of MC. A high amount of Mo has the opposite effect. The carbides that form by eutectic reaction increase in volume fraction with increasing C content, higher W/Mo ratio in the case of eutectic M6C, the V content9, and decreasing cooling rate. Many studies demonstrate how the as sintered microstructure of HSS can be tailored by means of addition of elemental powder to gas atomised M3/2 powder. The experiments include the addition of elemental Si to repel C from the melt when sintering, the addition of elemental Ni to avoid the formation of pearlite and stabilize austenite, and finally the addition of elemental V to form MC on the expense of cementite. Additions of carbides to high speed steels have been studied by a number of authors [9-19]. Thermodynamically less stable carbides (SiC, Cr_3C_2) easily dissolve in the high speed steel matrix during sintering or annealing and are not retained as discrete hard particles. Intermediate carbides such as WC, VC, Mo_2C and NbC, which include elements that are alloyed to high speed steel react with the steel matrix to produce new carbide phases with compositions similar to those of the normal primary carbides present in high speed steel, e.g M_6C {Fe_3W_3C or Fe_6Mo_3C} and niobium or vanadium rich MC type carbides. Thermodynamically stable carbides such as TiC are retained more less in their original form but also encourage MC carbides to form within the steel matrix and the steel/TiC interface because of some slight dissolution of the TiC particles. The TiC additions decreases sinterability by raising the sintering temperature required to achieve full density in a number of grades high speed steels, including M3/2. Most authors report also that the TiC addition reduces bend strength of the HSS and causes some slight increase in hardness.

The use of powder metallurgy PM techniques for manufacturing HSS is on the increase. In addition to the typical advantages of PM raw material savings, low energy costs. PM HSS present better microstructural features than conventional wrought steels homogeneity of carbide distribution in the matrix and smaller grain and carbide sizes, among others. These advantages mean an improvement of properties. PM techniques allow a higher content of alloying elements and the addition of the ceramic particles previously mentioned. If conventional compacting or CIP is used as the powder forming technique, a sintering process is then necessary. Sintering is usually carried out under vacuum conditions at temperatures below solidus temperature, although nitrogen-based atmospheres can sometimes be used, but this process does not completely eliminate porosity. A technique that provides densities as high as HIP but at a lower cost is liquid phase sintering. Liquid phase can be obtained in three ways:

1. by addition of a compound with a lower melting point than the material to be sintered, or that forms a eutectic,
2. by supersolidus sintering, which consists of heating to temperatures above the solidus temperature of the material to be sintered,
3. by infiltration technique [20, 21].

Infiltration is basically defined as "a process of filling the pores of a sintered or unsintered compact with a metal or alloy of a lower melting point." In the particular case of copper infiltrated iron and steel compacts, the base steel matrix, or skeleton, is heated in contact with the copper alloy to a temperature above the melting point of the copper, normally within the range of 1095° to 1150°C [22, 23]. Through capillary action, the molten copper alloy is drawn into the interconnected pores of the skeleton and ideally fills the entire pore volume. Filling of the pores with higher density copper can result in final densities in excess of 95% of the composite theoretical value. Completely filled skeletons also allow for secondary operation such as pickling and plating without damaging the structure through internal corrosion. Pressure tight infiltrated components are also possible for specific applications that demand the absence of interconnected porosity. The infiltration process is generally subdivided into two fundamental methods: single step or double step. The single step or single pass is presently the preferred infiltration method that consists of one run or passes through the furnace. In this process, the unsintered (green) steel and copper alloy compacts are placed in contact prior to furnace entry. The typical arrangement is to place the copper alloy infiltrant compact on the top surface of the steel compact. In some cases, it is preferred to place the steel compact on top of the infiltrant compact, or, infiltrate from top and bottom simultaneously. During the full furnace cycle, the steel base compact is ideally partially sintered prior to attaining the melting points of the infiltrant composition. Preferably, multi-independent zone furnaces are employed allowing for preheat, or lubricant burn-off, followed by pre-sintering (graphite solution) and finally infiltration. The double step or double pass infiltration method consists of pre-sintering or full sintering of only the steel compact in one pass through the furnace. After the first sintering pass, the unsintered (green) infiltrant compact is placed in contact with the sintered steel part, and the full furnace cycle is repeated. The infiltrating powders available may be used for both the single and double step processes. Most, if not all, infiltrating powders are prepared as a pre-blended and/or a pre-lubricated lot or batch and are designed for typical compacting operations. Shapes of infiltrant compact forms vary substantially depending upon the amount required and the configuration of the steel skeleton. Usually, simple infiltrant shapes, such as bars, cylindrical slugs, or annuli are compacted to a specific weight and are placed on the iron components in single or multiple contact arrangements.

The M3/2 high speed steel reinforced with tungsten carbide and infiltrated with copper was chosen for this investigation. The present paper describes and discusses the microstructural characteristics and mechanical behaviour of the composite system M3/2-WC-Cu.

2. Experimental procedure

2.1. The powders

Water atomised M3 grade 2 powder of - 160μm were obtained from POWDREX SA in the annealed condition. This powder was chosen, in preference to the more commonly used M2, for its better compressibility and sinterability. Chemical composition of this powder is given in the Table 1. As reinforcement's commercial tungsten carbides of - 3μm were used. The powder properties, including electrolytic copper are given in Table 2.

compound	C	Cr	Co	Mn	Mo	Ni	Si	V	W	Fe	O
composition	1,23	4,27	0,39	0,21	5,12	0,32	0,18	3,1	6,22	rest	626ppm

Table 1. Chemical composition of M3/2 HSS powders, wt-%

Powder properties	M3/2	WC	Cu
Bulk density, g/cm^3	2,26	2,70	1,60
Flow time, s/50g	38,5	-	-
Densification at 600MPa, g/cm^3	6,08	6,71	6,90
Particle size, μm	0÷160	0÷3	0÷40

Table 2. Properties of the used powders

The powders morphology is shown in fig 1.

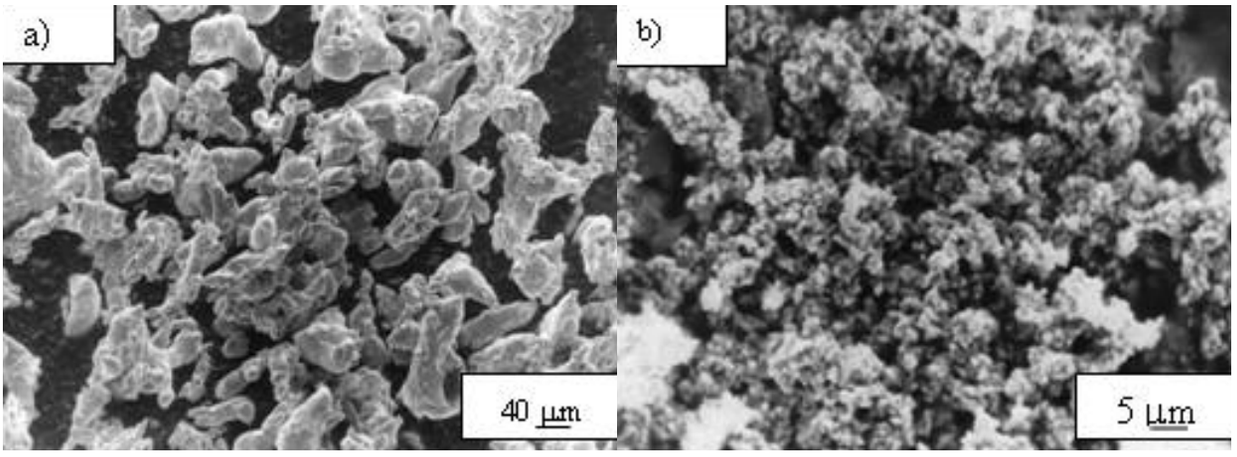

Figure 1. Scanning electron microscopy (SEM) morphology of powder particles:
a) high speed steel M3/2 class, b) tungsten carbides WC

It can be seen that the microstructure of the M3/2 grade HSS powders consists of a thin carbides in a martensitic-bainitic matrix. MC carbides being the white ones, Chile M C carbides are grey. Typical microhardness values for a powder is $\mu HV_{0,065} = 284 \pm 17$.

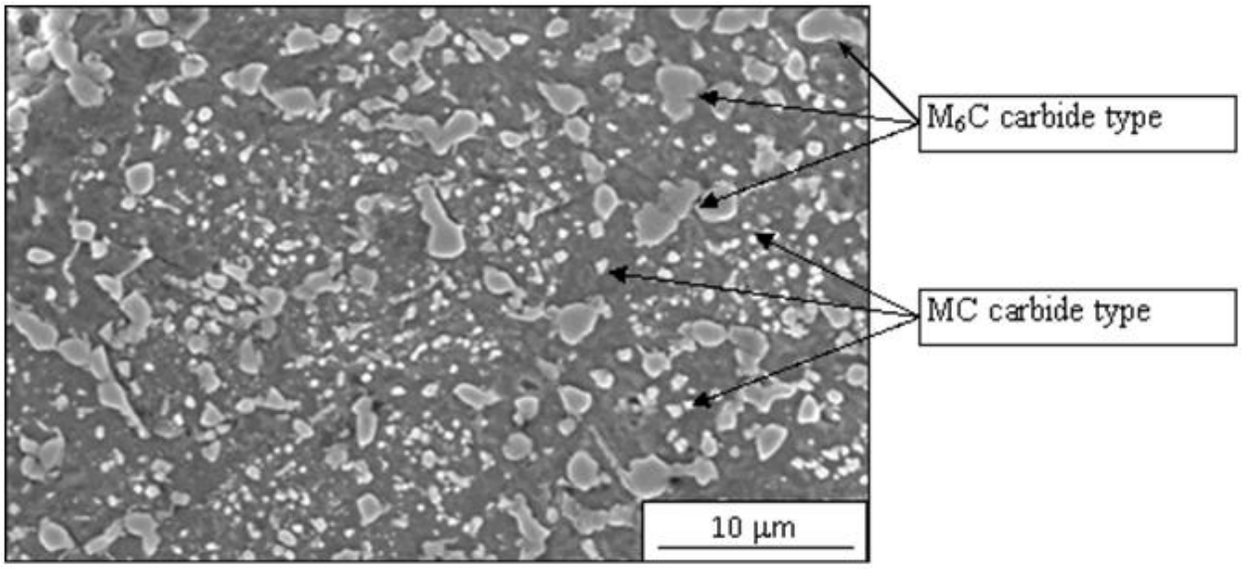

Figure 2. The microstructure of M3/2 grade HSS powder, SEM

2.2. Experimental technique

The compositions of powder mixtures are:

1. 100% M3/2,
2. M3/2 + 10% WC,
3. M3/2 + 30%WC.

Composite mixtures were blended in a Turbula® T2F blender for 30 min. The M3/2 powder and composite powders were uniaxially cold compacted in a cylindrical die at 800 MPa.

The infiltration process is subdivided into two fundamental methods: single step or double step. In the single step the unsintered (green) high speed steels or composite mixtures and copper alloy compacts were placed in contact prior to vacuum furnace entry. The copper alloy infiltrant compacts were placed on the top surface of the green compacts. The double step infiltration method consists of pre-sintering of only the green compacts. After the first sintering process, the infiltrant compacts (specify weight copper green compacts) were placed on the top surface of the sintered composites and were placed to vacuum furnace entry.

Half of green compacts were sintered in vacuum at 1150°C for 60 minutes. Sintered specimens and green compacts were analysed before infiltration. Density measurements via the Archimedes method were used to define the level of porosity.

Thereby obtained skeletons were subsequently infiltrated with copper, by gravity method, in vacuum furnace at 1150°C for 15 minutes. The infiltrated composites were cooled as fast as vacuum furnace.

The sintering and infiltration process was carried out in vacuum better than 10^{-2} Pa.

Densities of sintered materials were evaluated by a method based on the Archimedes principle, according to MPIF standard 42. Measured values were compared with theoretical

values to obtain relative densities (ρ_t). The theoretical densities for the composites were calculated according to the expression (1):

$$r_t = (r_a \times X_a + r_b \times X_b) \quad (1)$$

where ρ_a is carbide density, X_a the volumetric fraction of WC carbide, ρ_b the density of high speed steel M3/2, and X_b the volumetric fraction of the HSS.

The MMC composites materials were characterized using various techniques. The infiltrated specimens were subsequently tested for mechanical properties. Therefore, mechanical properties were characterized by Brinell hardness, wear resistance test and three points bend tests in order to determine the influence of tungsten carbide. The microstructure of the composites was examined by means of both light microscopy (LM) and scanning electron microscopy (SEM). Characterization of microstructures and the identification of phases present were performed by both optical and scanning electron microscopy, assisted by the use of X-ray energy dispersive analysis (EDX), backscattered electron image contrast, and some X-ray diffraction data. Reaction temperatures were determined by dilatometric study.

The wear tests were carried out using the block-on-ring tester (Figure 3).

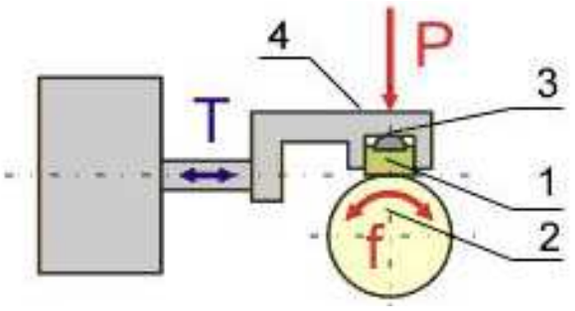

Figure 3. Tribosystem T05 - wear test principle

During the test a rectangular wear sample (1) was mounted in a sample holder (4) equipped with a hemispherical insert (3) ensuring proper contact between the test sample and a steel ring (2) rotating at a constant speed. The wear surface of the sample was perpendicular to the loading direction. Double lever system was used to force the sample towards the ring with the load accuracy of ±1%.

The wear test conditions were:

- test sample dimensions: 20 x 4 x 4 mm,
- rotating ring: heat treated steel 100Cr6, 55 HRC, ø49,5 x 8 mm,
- rotational speed: 500 rpm,
- load: 165 N,
- sliding distance: 1000 m.

The measured parameters were:

- loss of sample mass,
- friction force *F* (used to calculate the coefficient of friction).

The friction coefficient was measured continuously during the test, and the wear coefficient was calculated by means of the following expression (2):

$$F = \frac{friction \cdot force[N]}{load[N]} \tag{2}$$

Wear tracks were analyzed by LM to clarify wear mechanisms.

3. Results and discussion

3.1. Characterization of porous skeletons

The combined effects of tungsten carbide content and powder processing route on the relative density and shrinkage of the porous skeleton are shown in Figure 4 and 5.

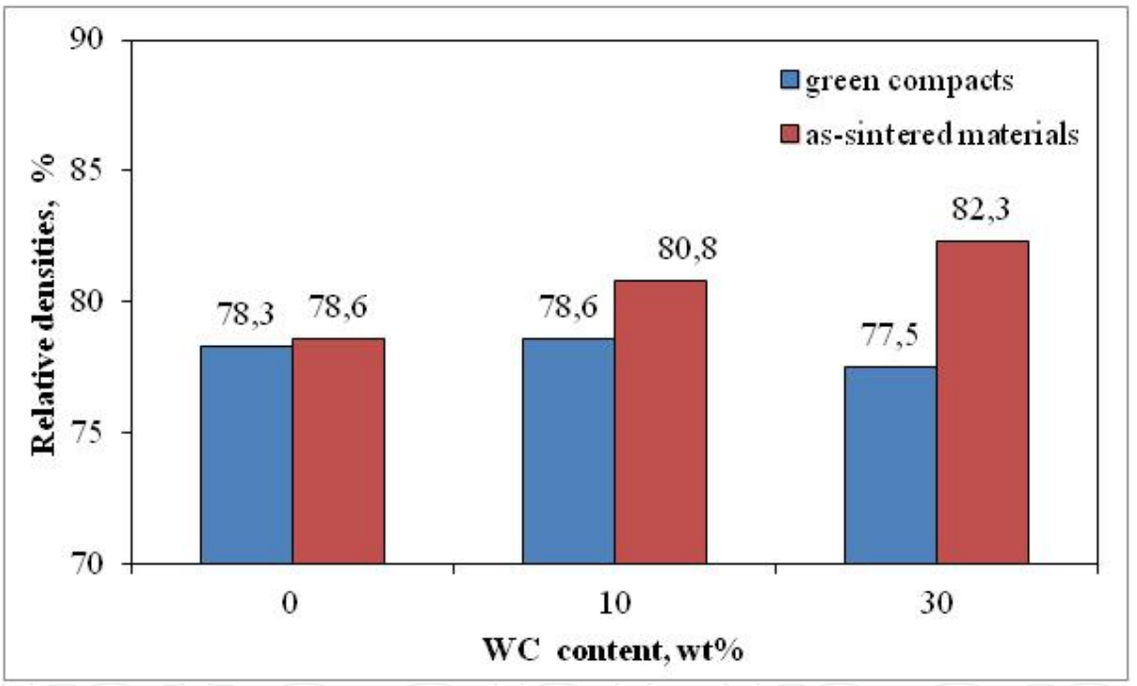

Figure 4. Relative densities of green compacts and pre-sintered porous skeletons as a function of tungsten carbide WC content

Figure 5 shows the effect of WC content on compressibility and shrinkage of high speed steel powders. It is evident that green density of compact decreases with increasing WC content. This attributes to hard and non-deforming nature of the tungsten carbide WC reinforcements, which constricts HSS-particle deformation, sliding and rearrangement during compaction. Additions of 30% tungsten carbide increase the as-sintered density.

Figure 4 shows that the M3/2 grade HSS cannot be fully densified at 1150°C, and that the as-sintered density is approximately equal to the green density. Additions of 30% tungsten carbide increase the as-sintered density presumably due to the occurrence of a liquid phase

resulting from a chemical reaction occurring between the HSS matrix and tungsten carbide particles. As exemplified in Fig. 6, marked specimen expansion followed by its rapid contraction has indicated that the chemical reaction takes place at temperatures between 1080 and 1110°C.

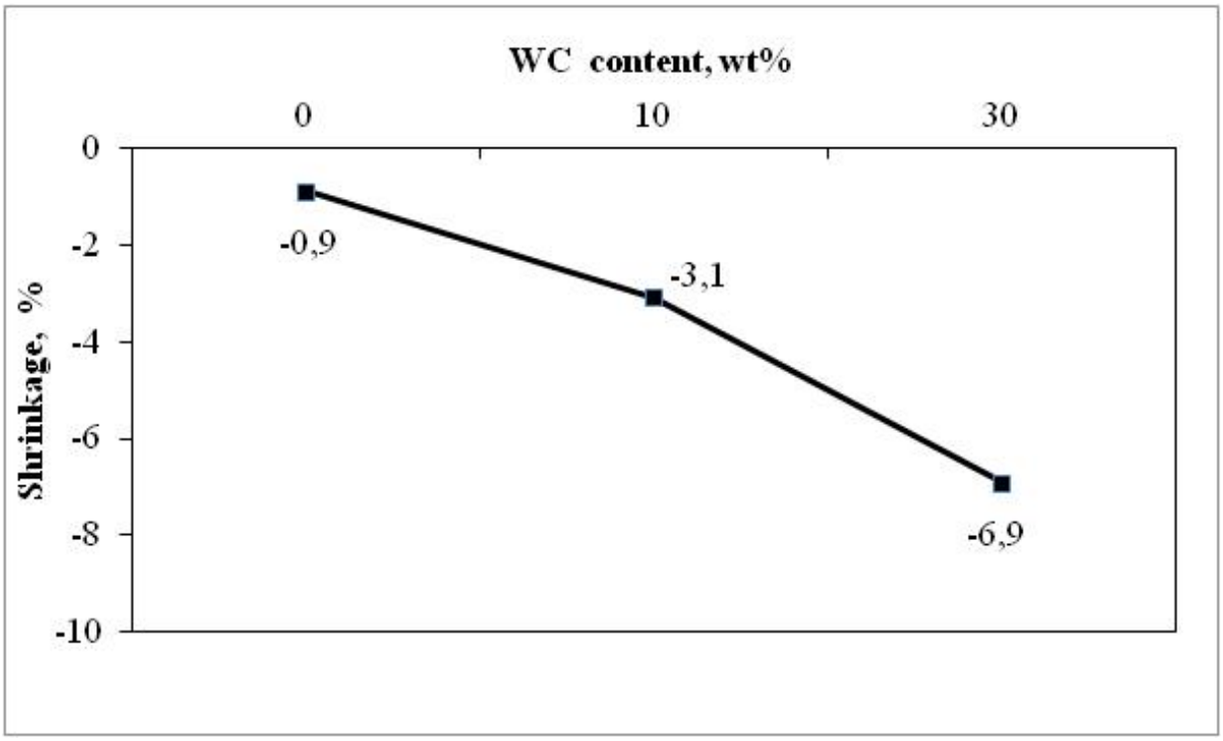

Figure 5. Shrinkage of compacts during sintering as a function of tungsten carbide WC content

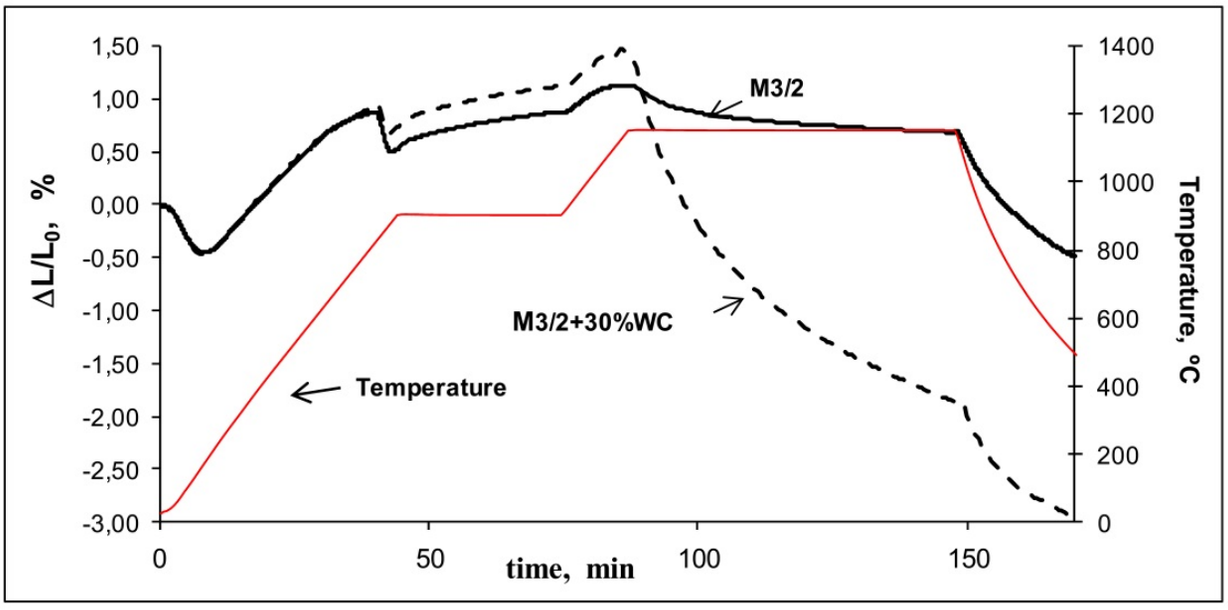

Figure 6. Dilatometric curves recorded on heating the M3/2 and HSS M3/2 + 30% WC material to the sintering temperature

Figures 4 and 5 show the morphologies of capillaries in both green compacts and pre-sintered skeletons.

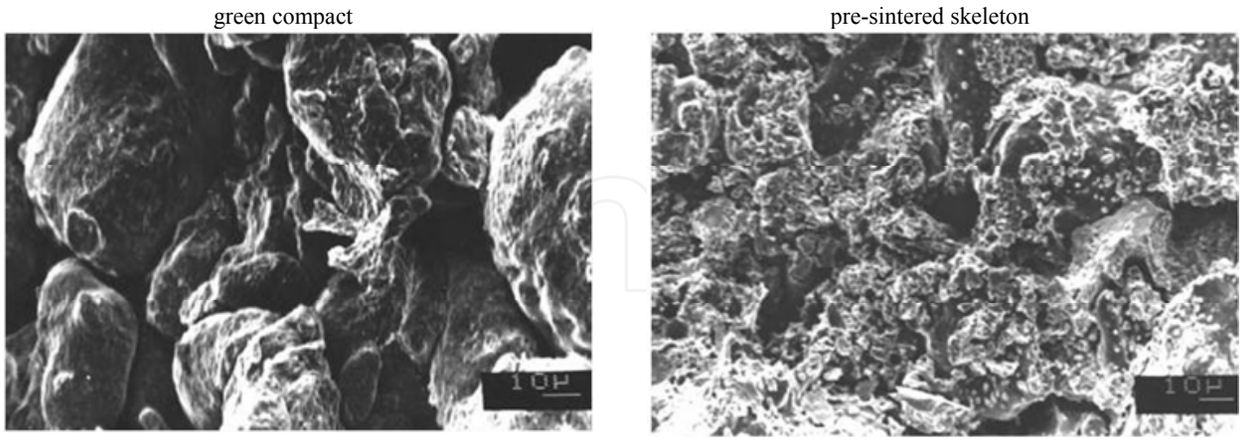

Figure 7. The morphologies of capillaries in M3/2 grade HSS, SEM

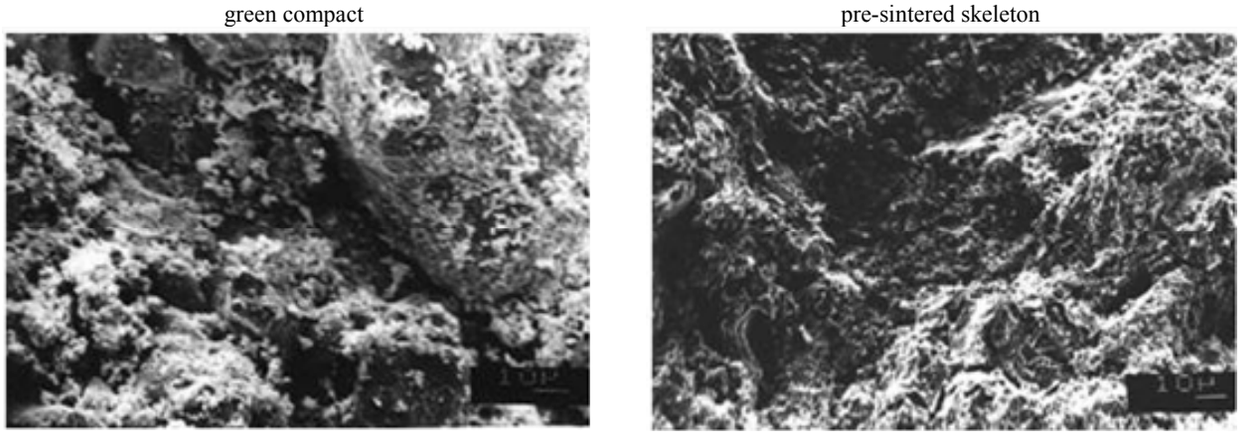

Figure 8. The morphologies of capillaries in M3/2 HSS + 30% WC , SEM

From the microstructural observations (Figures 7 and 5) it may be concluded that the morphologies of capillaries are mainly affected by the manufacturing route and powder characteristics (Fig. 1), such as powder particle size and morphologies of powder particles.

Finally, the porous skeletons were vacuum-infiltrated by gravity method at temperature: 1150°C for 15 min.

3.2. Characterization of as infiltrated materials

The as-infiltrated properties of the investigated composites are a complex function of the manufacturing route and tungsten carbide content. The properties of the as-infiltrated composites are shown in Figures 9÷12.

From Figure 9 it is evident that the molten copper is drawn into the interconnected pores of the skeleton, through a capillary action, and fills virtually the entire pore volume to yield final densities exceeding 97% of the theoretical value. In all cases, the additions of tungsten carbides aren't causes in the final density of the materials as compared with the base material.

Direct infiltration of as-sintered skeletons with copper results in the highest densities. This may be result of deoxidation powder particle surfaces during sintering in vacuum. Figure 10 show the final Cu content in as-infiltrated high speed steel based composites.

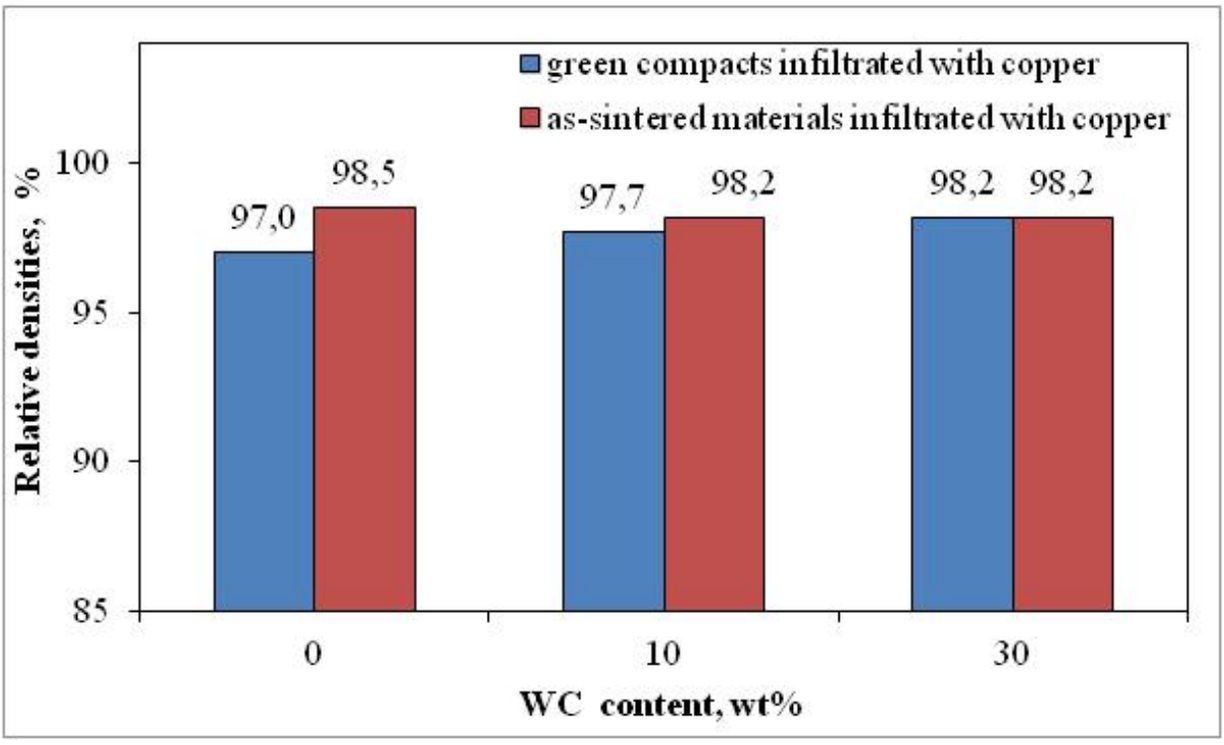

Figure 9. Relative densities of as-infiltrated composites

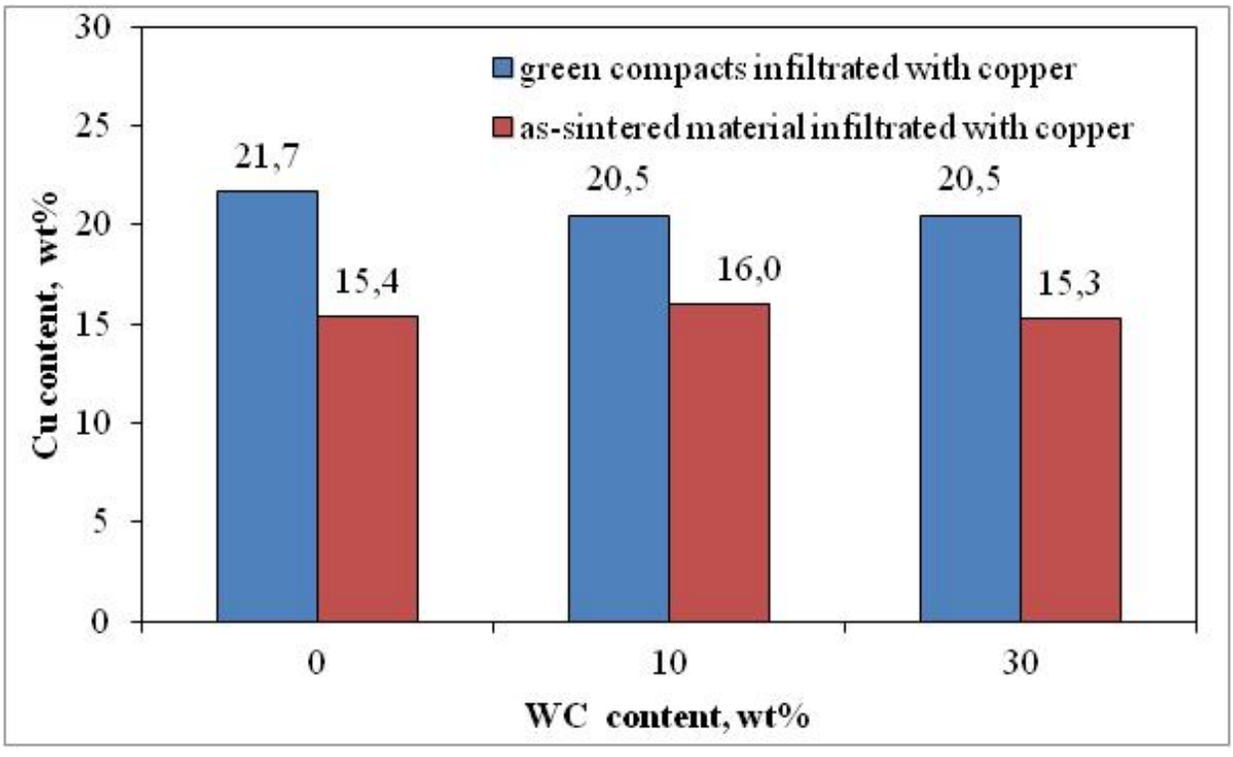

Figure 10. Copper content in as-infiltrated composites.

From Figure 10 it is evident that the copper content in as-sintered materials is lower than in infiltrated green compacts. It is affected by densification during sintering of porous skeletons.

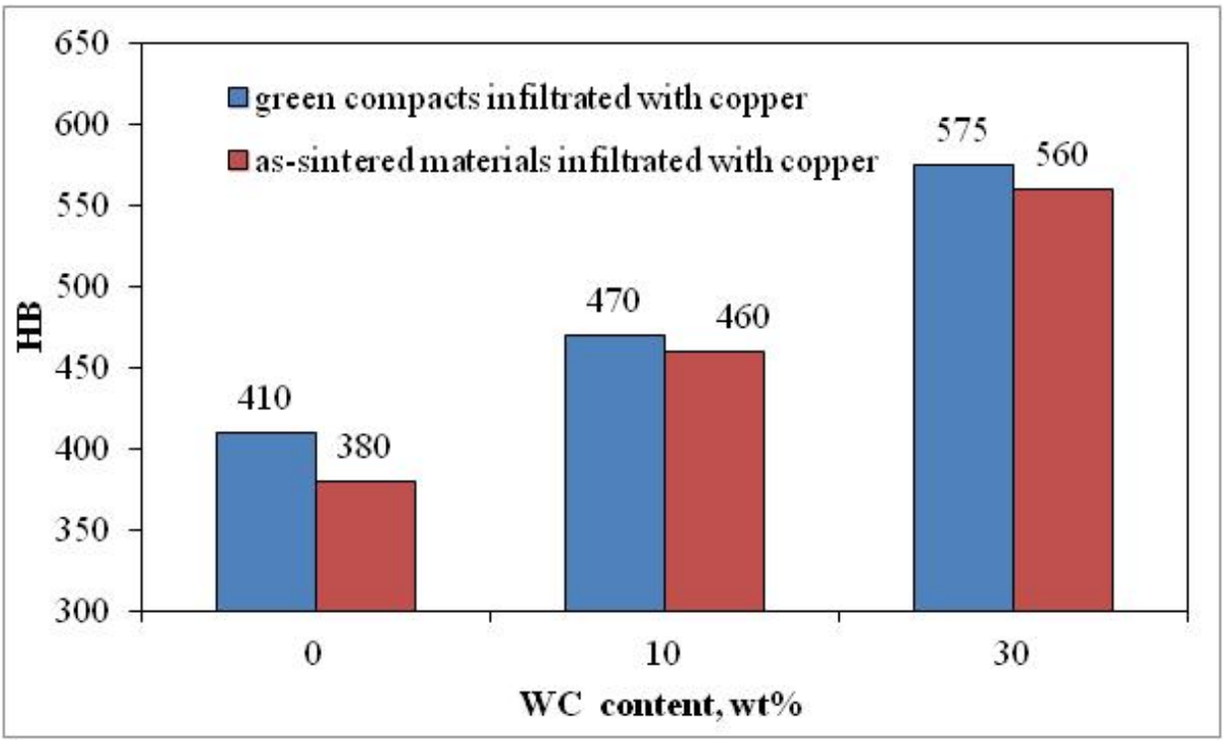

Figure 11. The Brinell Hardness of as-infiltrated composites

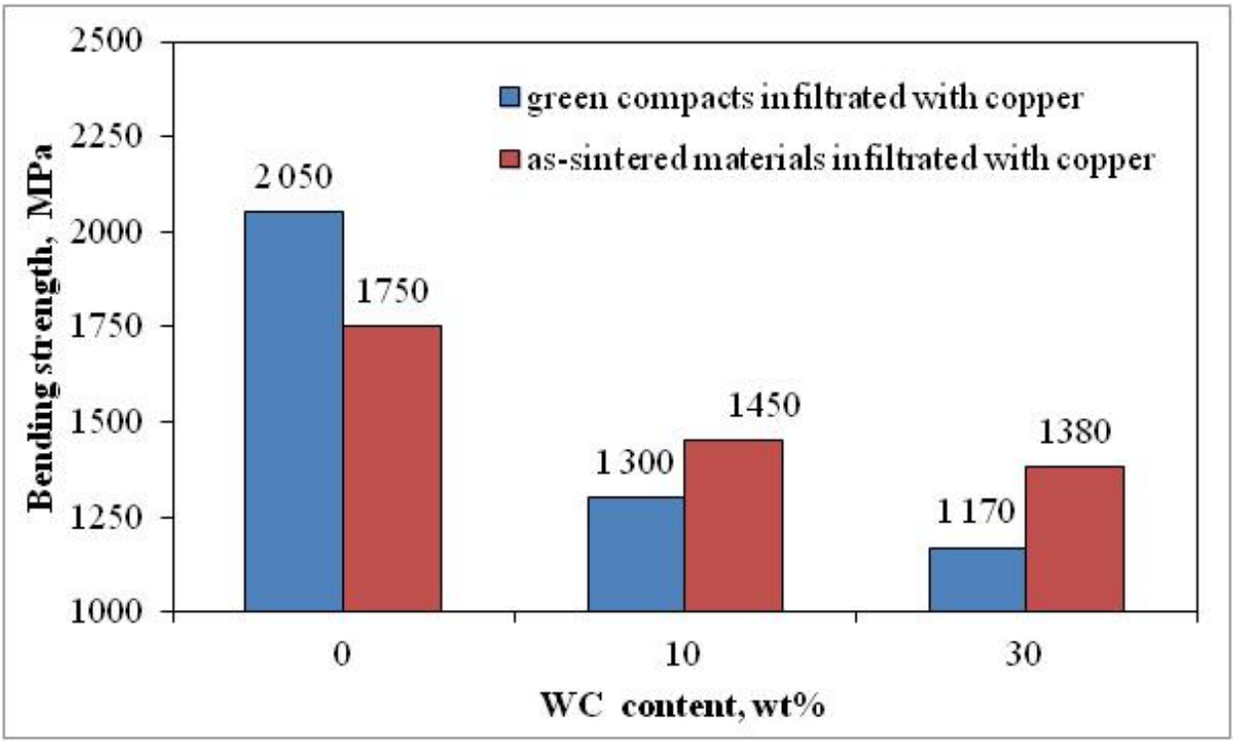

Figure 12. The Bending Strength of as-infiltrated composites

The Brinell hardness of the as-infiltrated composites increases with the percentage of additions of tungsten carbide WC. Considerable differences in hardness between the materials obtained from the two infiltration routes have been observed, with higher hardness numbers achieved with direct infiltration of green compacts, this can be explained by the diffusion of carbon and alloying of iron particles during sintering.

The Bending Strength of the as-infiltrated composites decreases with the increased content of tungsten carbide WC in the starting powder mix. For pre-sintered samples made of M3/2 – tungsten carbide mixture an increase of bending strength occurs; this can be explained by the chemical reaction between the tungsten monocarbide and HSS matrix.

3.3. Microstructures

Typical microstructures of a copper infiltrated green compact and pre-sintered skeleton are shown in Figures 13 – 15.

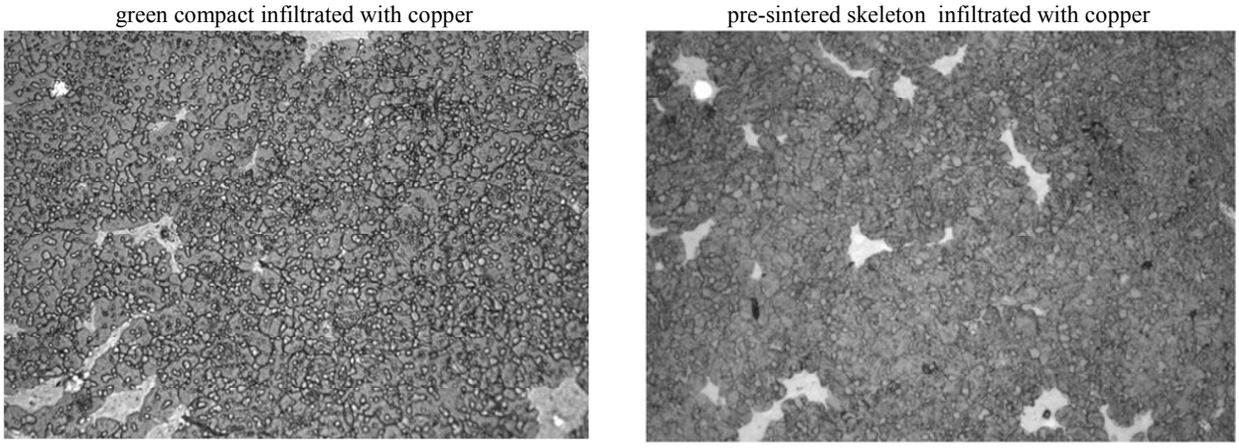

Figure 13. Microstructures of M3/2 HSS based composites

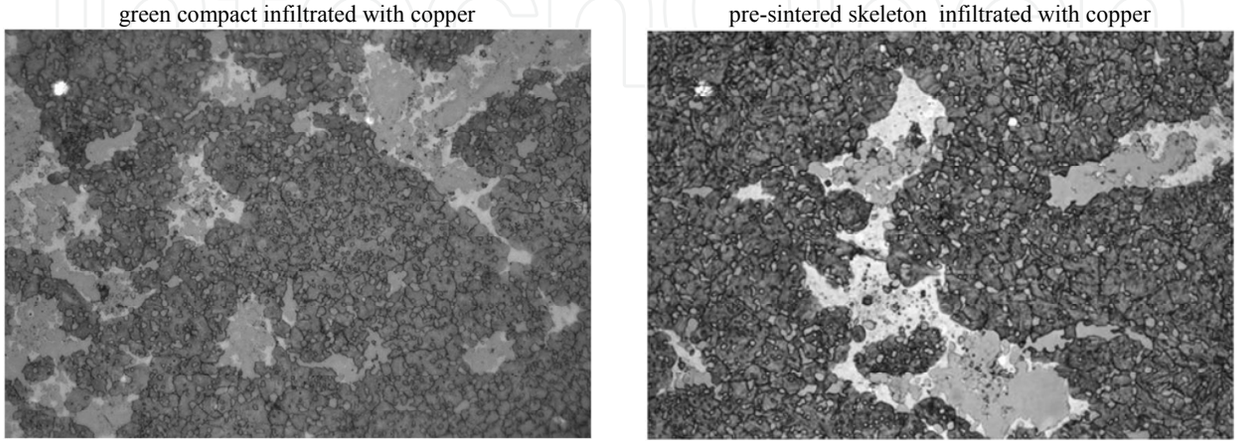

Figure 14. Microstructures of M3/2 HSS + 10%WC composites

It can be seen that the microstructure of the M3/2 grade HSS based composites consists of a steel matrix with finely dispersed carbides and islands of copper. Figures 13 and 15 shows tungsten carbides located within the grains and on the grain boundaries as well. Microstructures show small porosity at both sintering temperatures, and carbides are larger at the pre-sintered skeleton infiltrated with copper, MC carbides being the white ones, while MC carbides are grey. Some free copper areas are also present. In some places, these added carbides are related with white MC carbides, but free copper dark grey is preferentially linked to WC.

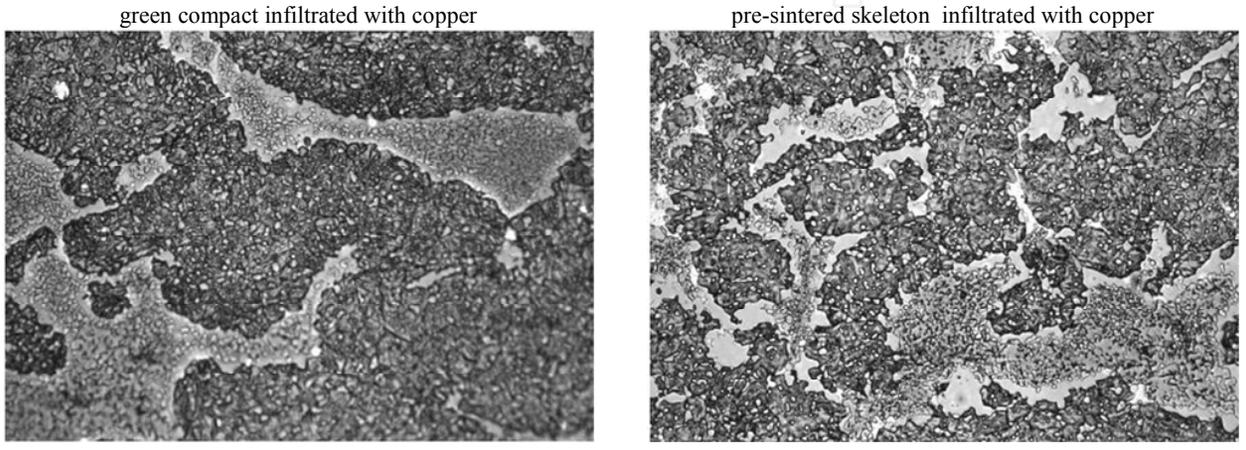

Figure 15. Microstructures of M3/2 HSS + 30%WC composites

SEM microstructures of a copper infiltrated green compact and pre-sintered skeleton are shown in Figures 16 – 17.

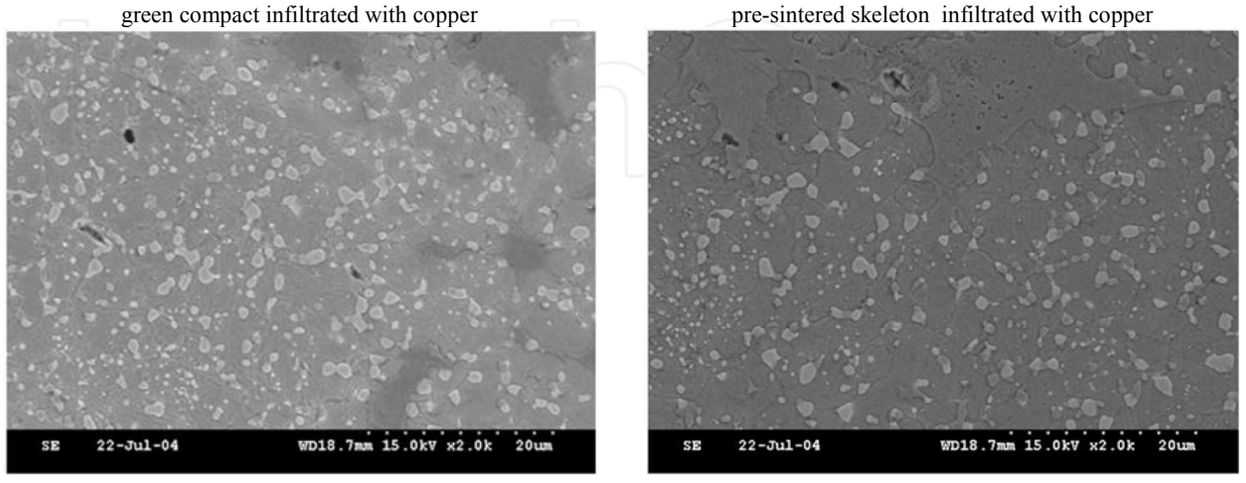

Figure 16. SEM microstructures of M3/2 HSS based composites

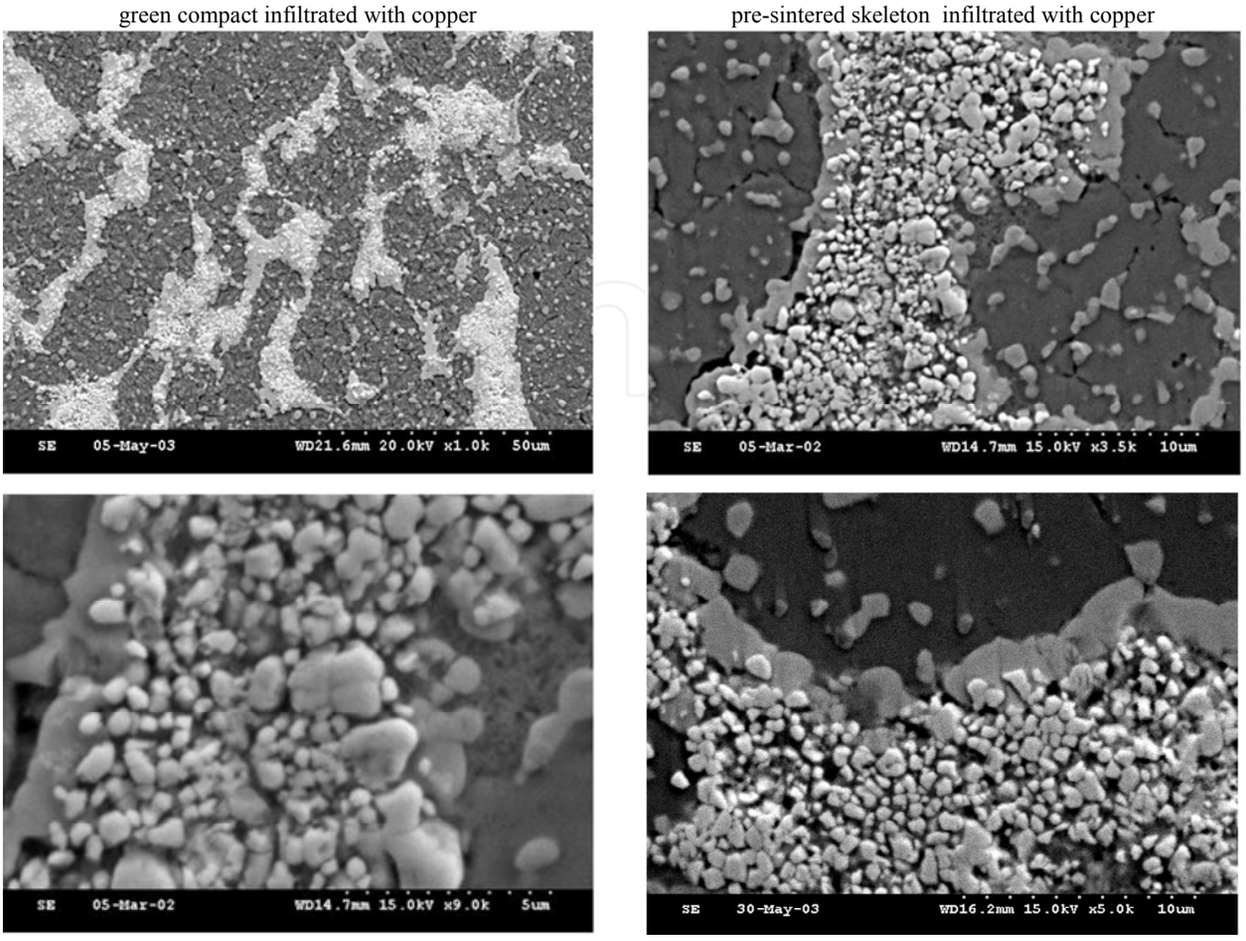

Figure 17. SEM microstructures of M3/2 HSS + 30%WC composites

4. Phase identification

Phase identification of the composites was performed by a Tur 62 X-ray diffraction (XRD) machine with Cu target (K_ω, λ = 1.5406Å).

Figure 19 show the XRD patterns of samples M3/2 + 30%WC. They illustrate the existence of the main carbides M_6C and MC as well as the existence of ferrite and austenite and the high intensity for the main Cu peak in sample green compact infiltrated with copper compared with sample pre-sintered skeleton infiltrated with copper as well as the higher intensity coming from higher volume of copper in as-infiltrated green compact. It should be noted that the intensity of the Fe_3W_3C peaks in sample pre-sintered skeleton infiltrated with copper can be explained by the chemical reaction between the tungsten monocarbide and HSS matrix.

The SEM and EDX analysis performed on the specimens containing M3/2 10 and 30% tungsten carbide have revealed the carbide phase evenly distributed within the copper-rich regions. As it is apparent from Figures 20 and 21, WC reacts with the surrounding HSS matrix and forms a tungsten and iron-rich M_6C carbide grain boundary network during sintering of porous skeletons.

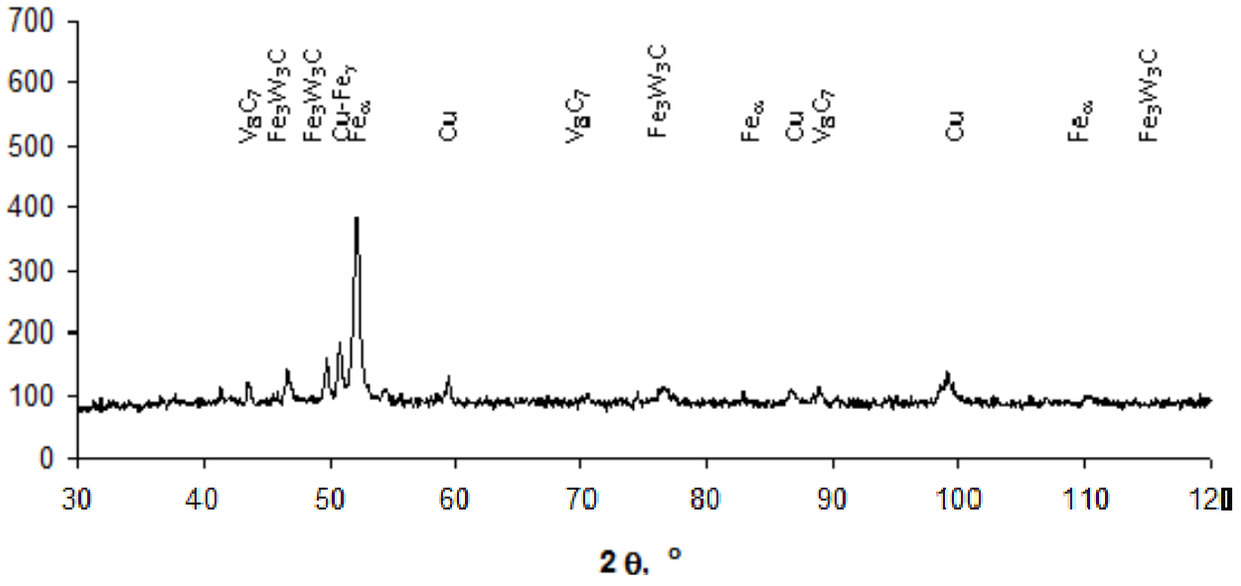

Figure 18. XRD pattern from M3/2 composites

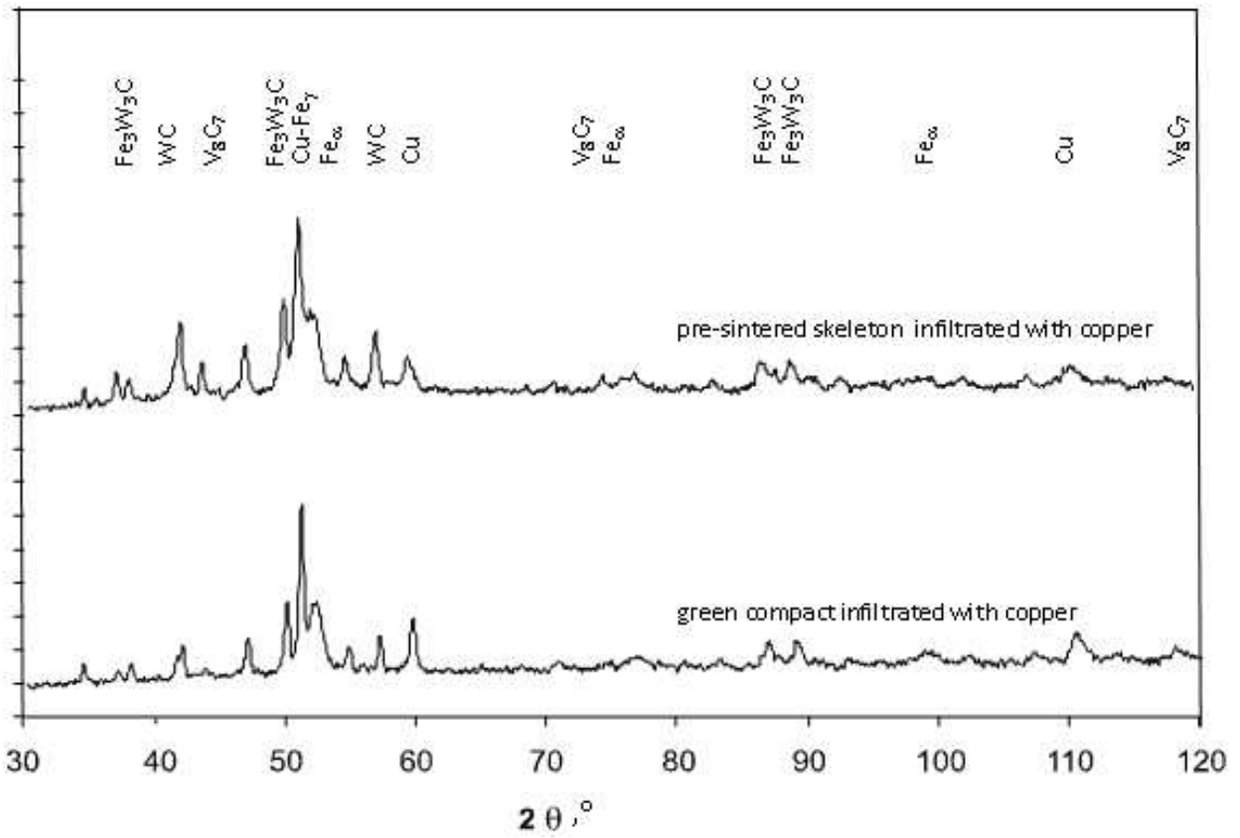

Figure 19. XRD pattern from M3/2 +30% WC composites

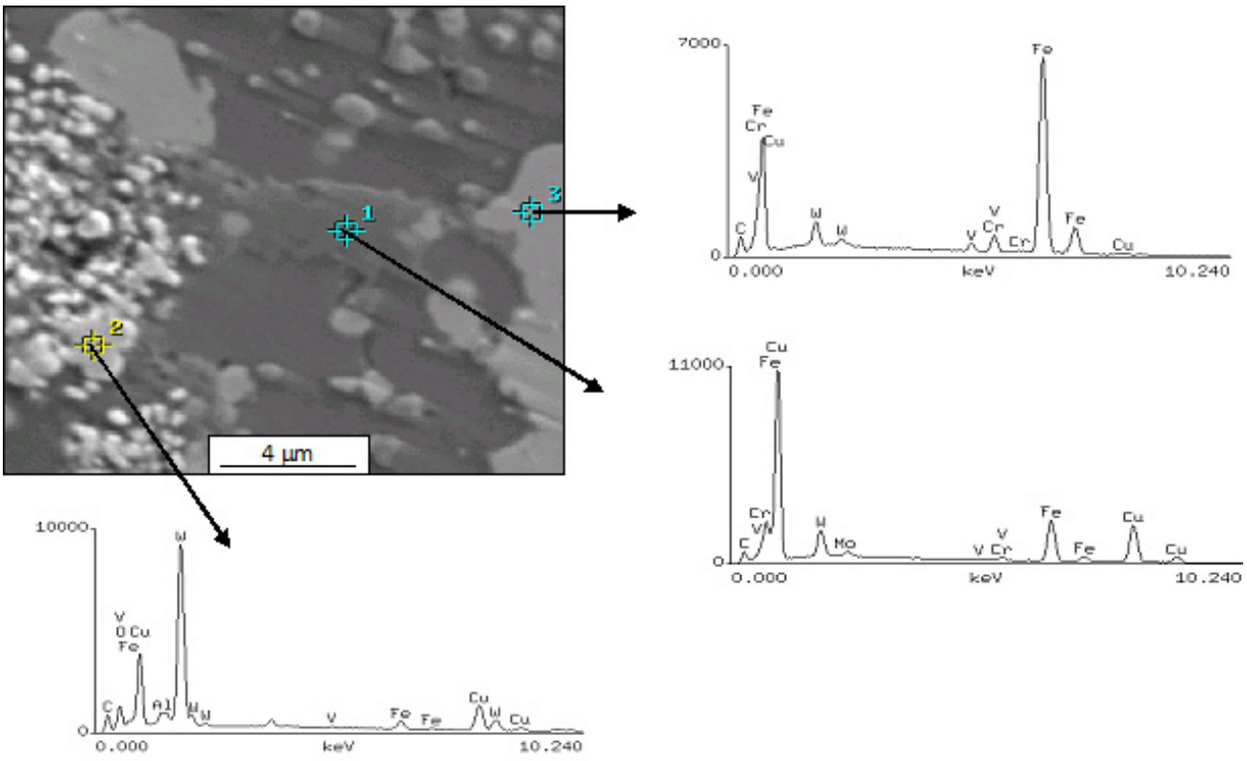

Figure 20. The microstructure of pre-sintered skeleton M3/2+30%WC infiltrated of copper and the qualitative EDX analysis, 1 – steel matrix, 2 – tungsten carbide WC, 3 – carbide M_6C type

Figure 21. The microstructure of pre-sintered skeleton M3/2+30%WC infiltrated of copper and the qualitative EDX analysis, 1 – steel matrix, 2 – carbide M_6C type

Intermediate carbides such as WC which include elements that are alloyed to high speed steel react with the steel matrix to produce new carbide phases with compositions similar to those of the normal primary carbides present in high speed steel, e.g M_6C {Fe_3W_3C }. The EDS analysis was carried out on sample pre-sintered skeleton M3/2+30%WC infiltrated of

copper to illustrate the chemistry of this carbides. Figure 22 shows elemental intensity maps for the alloying elements Fe, W and Cu. Most Fe is found in the matrix and grey M_6C carbides, while W is found in the whitish M_6C carbides. From Figure 21 it also evident that copper diffuse to steel matrix.

The carbide agglomerations observed are due to the non-assisted system used for mixing the powders; they could be avoided by using a more eficient mixing system such as a ball mill.

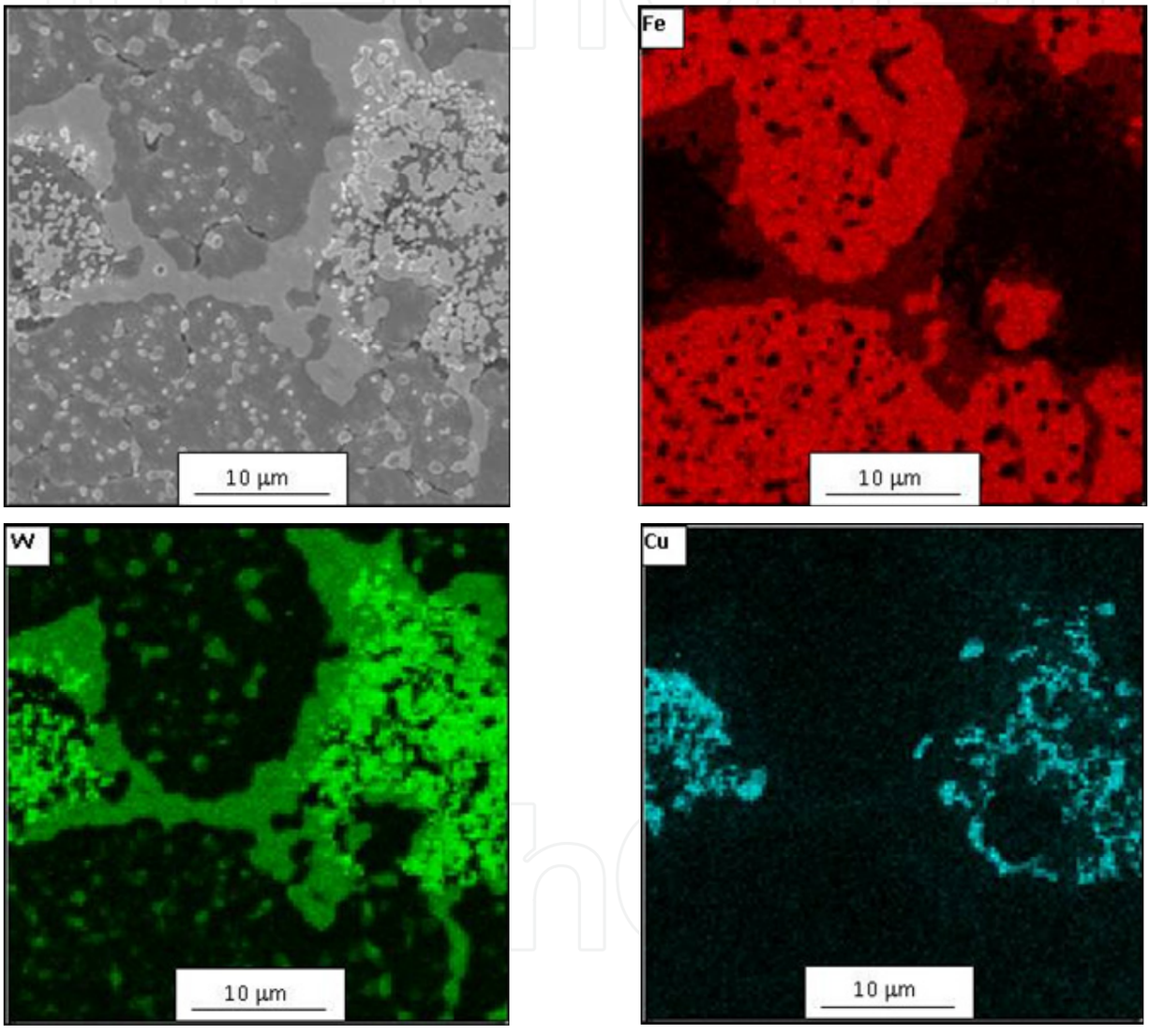

Figure 22. SEM micrograph and corresponding EDS maps of pre-sintered skeleton M3/2+30%WC infiltrated of copper

4.1. Tribological properties

All the specimens were polished to an average roughness of R_a = 1 µm. The tests were carried out at room temperature, keeping a relative humidity below 30%. The wear test results are given in Figures 23 and 24.

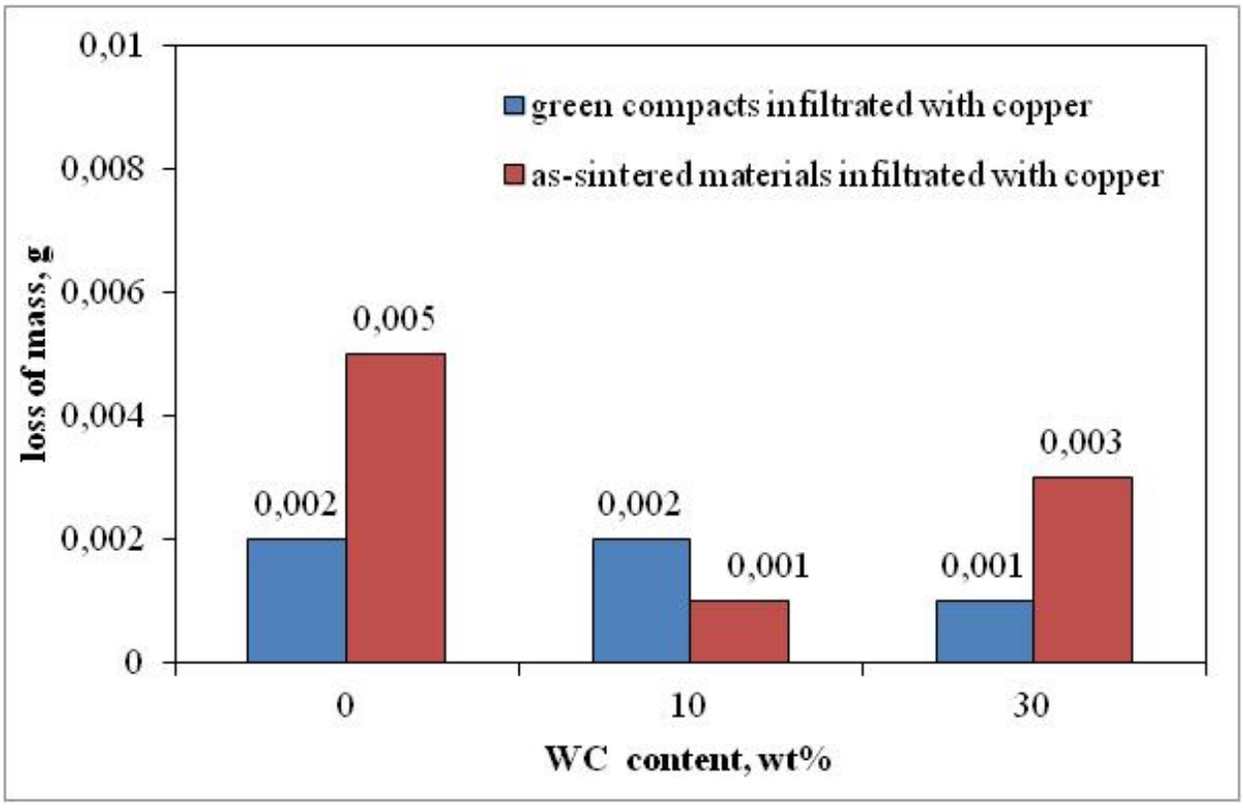

Figure 23. Loss of mass of as infiltrated composites

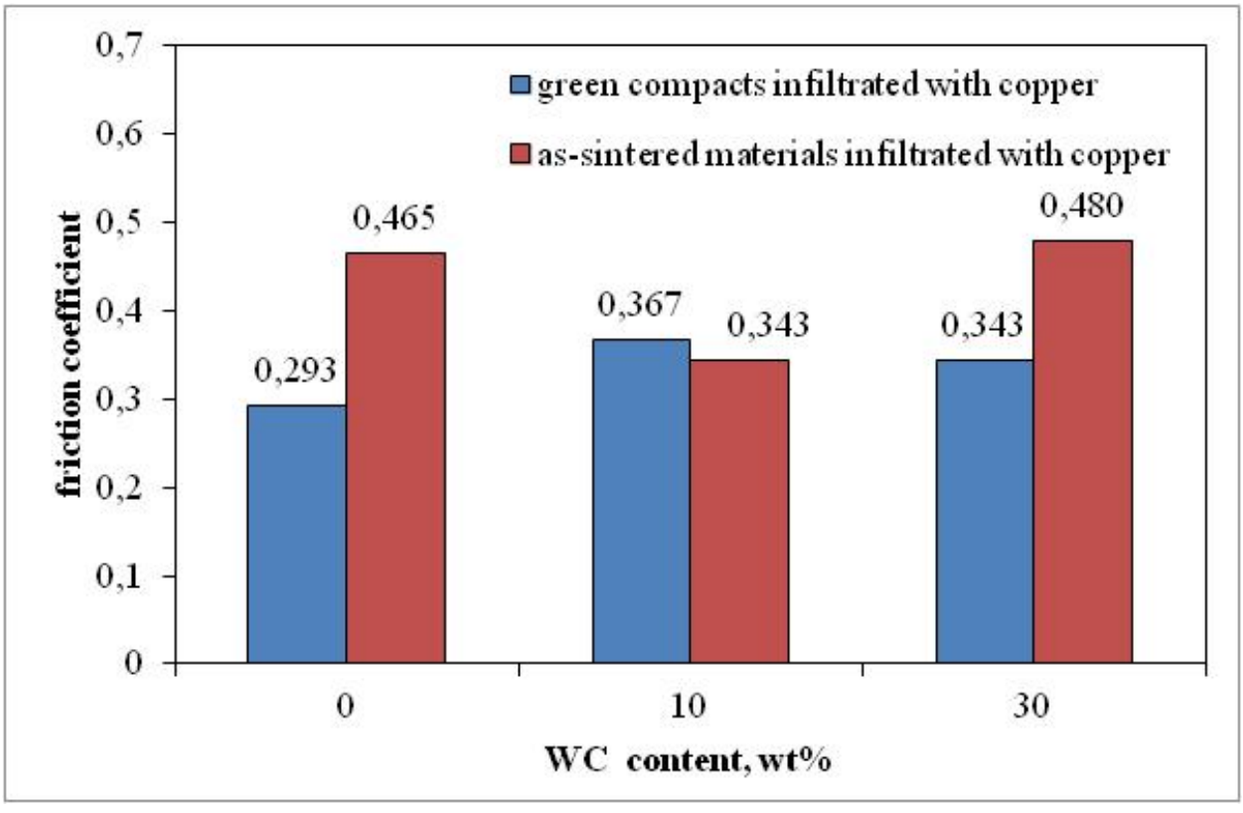

Figure 24. Friction coefficient of as infiltrated composites

The measurements of the wear resistance and friction coefficient permit classification of the as-infiltrated composites with respect to their tribological properties. Direct infiltration of green compacts with copper results in the highest wear resistance and almost the same friction coefficient of the as-infiltrated M3/2 and M3/2+30% WC composites. By comparing the wear resistance of composites received through direct infiltration of green compacts and infiltration of pre-sintered skeletons it is evident that the green compacts M3/2 and M3/2+30%WC compositions show 2÷3 times higher loss of mass than the tungsten carbide containing as-sintered materials infiltrated with copper. This can be explained by the diffusion of carbon and alloying of iron particles during sintering and chemical reaction between the tungsten monocarbide and HSS matrix. Friction coefficients are not highly influenced by the tungsten carbide additions, but the additions of 30% WC to high speed steel and infiltration with copper increase the wear resistance of these composites comparing to base material (M3/2 HSS infiltrated with copper). Wear tracks were analyzed by SEM to clarify wear mechanisms. Characteristic surface topographies after the wear test are exemplified in Figures 25 and 26.

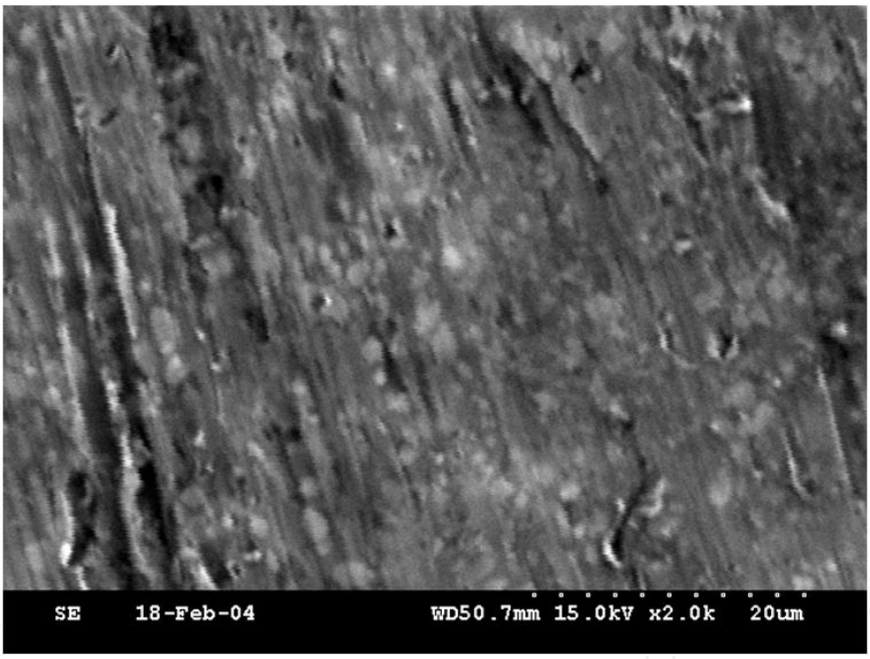

Figure 25. The surface of the as-infiltrated M3/2 composites after examining the wear resistance

The surface topographies of M3/2 and M3/2+30%WC specimens indicate occurrence of different wear mechanisms (Figure 25 and 26). In Fig. 25, typical abrasion scratches are seen in the base material. As a result of abrasion, ferrous oxides are generated and then dispersed through the wear track. The carbides seen on the wear-surfaces are being crushed and pulled out of the matrix to act as abrasive particles which increase the coefficient of friction. Figure 25 provide evidence of ploughing and sideways displacement of material in M3/2. Figure 26 shows smearing of iron oxides over the surface of the as-infiltrated M3/2+30%WC

composite which implies marked contribution of adhesive wear, whereas the extensive formation of iron oxides may account for the higher friction coefficients. In MMCs, the level of oxidation is lower than in plain steel. The best behaviour is observed for composite green compact M3/2+30%WC infiltrated of copper. These carbides are well linked to the matrix and cannot be easily detached. M_6C formed as a result of chemical reaction between additions of WC and steel matrix are affected by abrasion, while MC carbides remain in the matrix withstanding wear and creating barriers where oxides from matrix debris are accumulated. WC forms large size agglomerates of small particles, which are detached when abraded and spread across the wear track. At first, these particles act as abrasives, promoting three-body wear behavior. The infiltration of green compacts has two effects: on one hand, fewer particles are detached from the carbide clusters, and on the other hand, these particles are not encrusted in the matrix, producing three-body abrasion in all compositions.

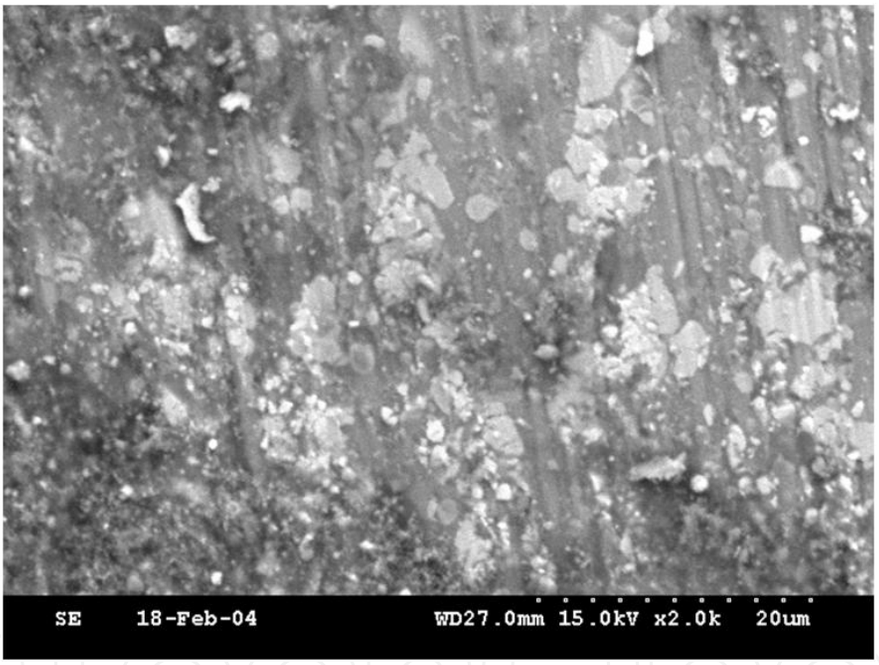

Figure 26. The surface of the as-infiltrated M3/2+30%WC composites after examining the wear resistance

The best materials from the viewpoint of mechanical properties were tested for wear properties is green compact M3/2 +30% tungsten carbide WC infiltrated with copper. Figures 23 and 24 suggest that, from the viewpoint of wear behaviour, the 30% reinforcement is the optimal composition for this type of composites.

5. Conclusions

1. Infiltration of porous HSS skeleton with liquid copper has proved to be a suitable technique whereby fully dense HSS based materials are produced at low cost.

2. Direct infiltration of green compacts with copper results in the higher hardness and higher resistance to wear of the M3/2 and M3/2+30 %WC composites, and allows to cut the production cost.
3. The mechanical properties of the HSS based composites are strongly dependent on the tungsten carbide content. The additions of tungsten carbide increase the hardness of HSS based composites, but decrease their bending strength.
4. Tungsten-rich M_6C type carbide is formed as a result of the chemical reaction between the tungsten monocarbide and HSS matrix
5. The carbides seen on the wear-surfaces of as infiltrated composites are being crushed and pulled out of the matrix to act as abrasive particles.

Author details

Marcin Madej
AGH University of Science and Technology,
Faculty of Metal Engineering and Industrial Computer Science, Krakow, Poland

Acknowledgement

This work was financed by Ministry of Science and Higher Education through the project No 11.11.110.788.

6. References

[1] Greetham G.: Development and performance on infiltrated and non-infiltrated valve seat insert materials and their performance. Powder Metallurgy, 1990, vol 3, no 2, pp. 112-114.
[2] Rodrigo H. Plama: Tempering response of copper alloy-infiltrated T15 high-speed steel, The International Journal of Powder Metallurgy, 2001, Vol. 37, No 5, s. 29-35.
[3] Wright C.S.: The production and application of PM high-speed steels. Powder Metallurgy 1994 vol 3, pp. 937-944.
[4] Torralba J.M. G. Cambronero, J. M. Ruiz-Pietro, M. M das Neves: Sinterability study of PM M2 and T15 HSS reinforced with tungsten and titanium carbides, 1993, vol 36, pp. 55 – 66.
[5] M. Madej, J. Leżański: Copper infiltrated high speed steel based composites, Archives of Metallurgy and Materials, 2005 vol. 50 iss. 4 s. 871–877.
[6] M. Madej, J. Leżański: The structure and properties of copper infiltrated HSS based, Archives of Metallurgy and Materials, 2008, vol. 53, iss. 3 s. 839–845.
[7] M. Madej: The tribological properties of high speed steel based composites, Archives of Metallurgy and Materials 2010 vol. 55 iss. 1 s. 61–68

[8] L.A. Dobrzanski, [..]: Fabrication methods and heat treatment conditions effect on tribological properties of high speed steels, Journal of Metarials Processing Technology, 157-158, (2004), s. 324-330.
[9] E. Gordo, F. Velasco, N. Anto´n, J.M. Torralba: Wear mechanisms in high speed steel reinforced with (NbC)p and (TaC)p MMCs, Wear 239 (2000), s. 251–259
[10] Farid Akhtar: Microstructure evolution and wear properties of in situ synthesized TiB2 and TiC reinforced steel matrix composites, Journal of Alloys and Compounds, 459 (2008), s. 491–497
[11] G. Hoyle: *High Speed Steels.* Butterworth & Co. Publishers. Cambridge 1998
[12] Shizhong Wei, Jinhua Zhu, Liujie Xu: Effects of vanadium and carbon on microstructures and abrasive wear resistance of high speed steel, Tribology International 39 (2006), s. 641–648
[13] Z. Zalisz, A. Watts, S.C. Mitchell, A.S. Wronski: Friction and wear of lubricated M3 Class 2 sintered high speed steelwith and without TiC and MnS additives, Wear 258 (2005), s. 701–711
[14] W. C. Zapata, C. E. Da Costa, J. M. Torralba: Wear and thermal behaviour of M2 high-speed steel reinforced with NbC composite, Journal of Materials science, 33 (1998) 3219 – 3225
[15] G. A. Baglyuk and L. A. Poznyak: The sintering of powder metallurgy high-speed steel with activating additions, Powder Metallurgy and Metal Ceramics, Vol. 41, No 7-8, 2002, s. 366-368
[16] W. Khraisat, L. Nyborg and P. Sotkovszki: Effect of silicon, vanadium and nickel on microstructure of liquid phase sintered M3/2 grade high speed steel, Powder Metallurgy 2005 Vol. 48 No. 1 s. 33-38
[17] J. A. Jime´nez, M. Carsı, G. Frommeyer and O. A. Ruano: Microstructural and mechanical characterisation of composite materials consisting of M3/2 high speed steel reinforced with niobium carbides, Powder Metallurgy 2005 Vol. 48 No. 4, s. 371-376
[18] J. D. Bolton and A. J. Gant: Phase reactions and chemical stability of ceramic carbide and solid lubricant particulate additions within sintered high speed steel matrix, Powder Metallurgy 1993 Vol. 36 No.4, s. 267-274.
[19] J. D. Bolton and A. J. Gant: Heat treatment response of sintered M3/2 high speed steel composites containing additions of manganese sulphide, niobium carbide, and titanium carbide, Powder Metallurgy 1996 Vol. 39 No.1, s. 27-34.
[20] M. Madej: Copper infiltrated high speed steel based composites with iron additions, Archives of Metallurgy and Materials, 2009 vol. 54 iss. 4 s. 1083–1091
[21] M. Madej: The tribological properties of high speed steel based composites, Archives of Metallurgy and Materials, 2010 vol. 55 iss. 1 s. 61–68
[22] H. G. Rutz and F. G. Hanejko: High density processing of high performance ferrous materials, international conference & Exhibition on powder Metallurgy & Particulate Materials, May 8-11, 1994 - Toronto, Canada

[23] M. M. Oliveira: *High-speed steels and high-speed steels based composites*. International Journal of Materials and Product Technology, 2000, Vol. 15, No 3÷5, s. 231-251.

IntechOpen